ELSEVIER

Chemical Engineering Journal 69 (1998) 7–20

Chemical Engineering Journal

A model of laminar micromixing with application to parallel chemical reactions

J. Bałdyga [a,*], A. Rożeń [a], F. Mostert [b]

[a] *Warsaw University of Technology, Warszawa, Poland*

[b] *DSM Research, Geleen, Netherlands*

Received 6 January 1996; revised 18 August 1997; accepted 26 August 1997

Abstract

The effect of laminar micromixing on parallel reactions was studied experimentally and interpreted theoretically using a new model of laminar micromixing, developed by applying an integral transformation to material balance equations in the Lagrangian frame of reference. A solution of sodium hydroxide was contacted with a premixture of hydrochloric acid and ethyl chloroacetate solutions in two reactors: a semibatch tank reactor and a twin-screw extruder. The viscosities of the mixed solutions were increased to 0.3 Pa s with polyethylenepolypropylene glycol to obtain a laminar flow regime in both reactors. The selectivity of the parallel reactions was then dependent on the mode of operation, intensity of mixing, initial stoichiometric ratio and volume ratio of the mixed solutions. The model was used to determine an energetic efficiency of mixing based on the results of the parallel reaction experiments; the procedure proposed enables a direct and strict comparison to be made of systems with different geometries and/or mode of operation. © 1998 Elsevier Science S.A.

Keywords: Energetic efficiency of mixing; Extruder; Laminar mixing; Parallel reactions; Semibatch reactor

1. Introduction

Processes of laminar mixing are met in practice when the liquids to be mixed are very viscous. These processes take place in numerous industrial applications, e.g., polymer production and processing [1,2], manufacturing of ceramics or glassware [3], food processing and production of biomass [4,5]. In general, when liquids are very viscous, the realization of a mixing operation faces serious problems, resulting from the fact that high inputs of mechanical energy or long mixing times are required [6–8]. Moreover, in the case of a reacting system the method of contacting the reagents, the number and kinetics of the chemical reactions and the method of mixing may influence the selectivity of the chemical reactions, the weight distribution of polymer molecules or the size distribution of particles. As a result, there is a need to develop a rigorous and general procedure, based on experimental data and mixing theory, for the determination of the energetic efficiency of mixing. Such a method can be used to compare the mixing efficiency of different systems and to establish a hierarchy of reactors or mixers from the viewpoint of efficient mixing. The mixing literature indicates that the strongest effect of mixing can be observed for multiple reactions with nonlinear kinetics carried out in nonpremixed feed systems [9–11]. When two or more streams of different reactants are introduced into a reactor, mixing of different species occurs as well as mixing of material elements of different ages. Mixing of species on the molecular scale must precede their reaction, which means that, in the case of an irreversible reaction between two nonpremixed feed reactants, the conversion for complete segregation in the reactor equals zero, whereas for maximum mixedness it approaches unity. The process of mixing on the molecular scale (micromixing) is the final stage in a sequence of mixing processes (macro-, meso- and micromixing [12]), and can dominate the course of the whole process, provided that the chemical reactions are relatively fast. It should also be noted that the mechanism of laminar mixing is complex, and many aspects of mixing are still not completely understood. Mathematical models of laminar mixing, available in the mixing literature, are usually based on simplified mixing mechanisms; therefore so their application is often limited and the range of application is not always clear.

An interpretation of laminar mixing as a process of continuous deformation increasing the contact surface area between

* Corresponding author. Warsaw University of Technology, Department of Chemical and Process Engineering, ul. Waryńskiego 1, 00-645 Warszawa, Poland. Tel.: +48-22-6606376; fax: +48-22-251440; e-mail: baldyga@ichip.pw.edu.pl

PII S1385-8947(97)00101-0

the fluids being mixed was proposed by Spencer and Wiley [13]. These workers emphasized the influence of orientation of the intermaterial surface in the flow field on the rate of mixing. These concepts were adopted by Mohr et al. [14,15], who defined a new quantity, 'a striation thickness', equal to the distance separating a pair of like interfaces, to measure the scale of segregation. It was shown how the striation thickness could be decreased in simple flows such as tensile deformation and shear flow [15]. The theory of Mohr was further developed by Ranz [16], Ottino et al. [17] and Ottino [18], who proposed a general relation for the rate of change of the intermaterial area and the striation thickness (defined as one-half of Mohr's striation thickness) in any flow field and formulated models of mixing including effects of molecular diffusion and chemical reactions. These workers [16–18] applied a Lagrangian approach to consider the history of mixing of a single fluid element. In the small fluid element, passing through various regions of the system, the flow field can be decomposed into a pure deformation and a 'rigid body' rotation [16]. The striation thickness and the intermaterial surface area change due to deformation. Following Ottino et al. [17], the rate of change of these quantities in the close proximity of a material point $\vec{X}$ reads

$$\alpha(\vec{X},t) = -\frac{1}{s}\frac{\partial s}{\partial t}\bigg|_{\vec{X}} = \frac{1}{a_v}\frac{\partial a_v}{\partial t}\bigg|_{\vec{X}} = \text{div}\,\vec{v} - \ddot{D}:\hat{n}\hat{n} \tag{1}$$

where $\ddot{D}$ denotes the symmetrical deformation tensor

$$\ddot{D} = \frac{1}{2}\left[\text{Grad}\,\vec{v} + (\text{Grad}\,\vec{v})^{\mathrm{T}}\right] \tag{2}$$

and $\hat{n}$ is the direction unit vector of a material line or plane; for incompressible fluids, Eq. (1) has a simpler form because div $\vec{v} = 0$.

By neglecting the variation of the species concentrations in planes parallel to the intermaterial surfaces, the material balance in a local frame of reference (ξ_1, ξ_2, ξ_3) with the j axis perpendicular to the contact surface, can be written as follows [17,18]

$$\frac{\partial c_i}{\partial t} - \alpha\xi_j\frac{\partial c_i}{\partial \xi_j} = D_i\frac{\partial^2 c_i}{\partial \xi_j^2} + R_i \tag{3}$$

The 'rigid body' rotation of the fluid caused by the nonvanishing rotation tensor

$$\ddot{\Omega} = \frac{1}{2}\left[\text{Grad}\,\vec{v} - (\text{Grad}\,\vec{v})^{\mathrm{T}}\right] \tag{4}$$

does not influence directly the process of mass transport, but can alter the orientation of the material line and so change the effective rate of deformation, $\alpha(\vec{X},t)$. Ottino et al. [17] determined the upper bound for the rate of deformation, which for incompressible and Newtonian fluids equals [17]

$$\alpha_{\max} = \sqrt{\ddot{D}:\ddot{D}} = \sqrt{\varepsilon/(2\mu)} \tag{5}$$

This allowed Ottino et al. [19] to include the effect of rotation on the rate of generation of the intermaterial surface area by a single scalar parameter—'the energetic efficiency of mixing'

$$\text{eff}(\vec{X},t) \equiv -\frac{\ddot{D}:\hat{n}\hat{n}}{\sqrt{\ddot{D}:\ddot{D}}} = \frac{\alpha}{\alpha_{\max}} = \frac{\alpha}{\sqrt{\varepsilon/(2\mu)}} \tag{6}$$

The relation between viscous deformation and molecular diffusion during mixing on a molecular scale has been proposed [16–18]. To illustrate this phenomenon, let us consider, as an example, the case of an instantaneous (completely controlled by mixing) reaction

$$\mathrm{A} + \mathrm{B} \xrightarrow{k\to\infty} \text{Products} \tag{7}$$

proceeding in three-dimensional space, in a two-dimensional stagnation flow

$$v_x = \alpha x,\ v_y = -\alpha y,\ v_z = 0 \tag{8}$$

Initially, N_{B0} moles of reactant B are concentrated at point $(x, y, z) = (0, 0, 0)$. The rest of the space is occupied by reactant A of initial concentration c_{A0}. Fig. 1 shows the time evolution of the intersection of the instantaneous reaction surface at plane $z = 0$ for both substrates of the same molecular diffusivity. For short times ($t \ll \alpha^{-1}$), the B-rich zone spreads solely as a result of molecular diffusion. However, as the time increases ($t > \alpha^{-1}$), the reaction zone becomes compressed in the y direction and drawn out in the x direction. The concentration gradient and the molecular diffusion are increased in the y direction and reduced in the x direction. Thus the process of molecular diffusion becomes one-dimensional and, because the increase in diffusion in the y direction is much larger than the decrease in diffusion in the x direction, deformation accelerates the process. The final shrinking of the reaction zone is due to chemical conversion.

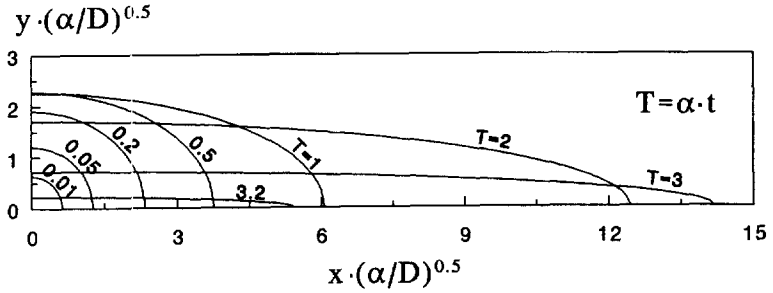

Fig. 1. Time evolution of an instantaneous reaction plane at $z = 0$; $\alpha D^{-1.5} N_{\mathrm{B0}} c_{\mathrm{A0}}^{-1} = 1000$.

These findings and the work described in Refs. [16–18] are the starting point for the present work, the main aims of which are to create a new model of laminar micromixing, to develop a reactive tracer method for the experimental investigation of micromixing, and finally, by combining the model and the experimental method, to propose a strict procedure which enables the energetic efficiency of mixing to be determined.

2. Theoretical details

The following considerations are restricted to the mixing of Newtonian, incompressible and completely miscible fluids of $Sc \gg 1$ (liquids) in single-phase systems (no interfacial tension) under isothermal conditions. The flow in the mixer or reactor is laminar and it is assumed that no flow instability arises during mixing. The viscosity and density of the mixed liquids, as well as the diffusion coefficients of the reactants and the chemical reaction rate constants, do not depend on the mixture composition.

Let us consider a fluid element containing a diffusive tracer (spot of contaminant), which is transported, deformed and rotated by surrounding fluid (Fig. 2). The differential mass balance in a local coordinate system (ξ_1, ξ_2, ξ_3) attached to the centre of mass of the spot reads

$$\frac{\partial c}{\partial t}+\sum_{i=1}^{3}\frac{\partial}{\partial \xi_i}\left[c u_i(\vec{\xi})\right]=D\sum_{i=1}^{3}\frac{\partial^2 c}{\partial \xi_i^2} \tag{9}$$

where $\vec{\xi}=\vec{x}-\vec{X}$ is the position vector in the moving frame. The fluid element is assumed to be always so small that relative motion $\vec{u}(\vec{\xi})=\vec{v}(\vec{x})-\vec{v}(\vec{X})-\vec{\omega}\times\vec{\xi}$ within this element can be regarded as linear

$$\vec{u}(\vec{\xi})=\mathrm{Grad}\,\vec{u}\,|_{\xi=0}\times\vec{\xi} \tag{10}$$

Using Eq. (10) and the continuity equation

$$\mathrm{div}\,\vec{u}=0 \tag{11}$$

we can transform expression Eq. (9) into

$$\frac{\partial c}{\partial t}+\sum_{i=1}^{3}\sum_{j=1}^{3}\xi_j\frac{\partial u_i}{\partial \xi_j}\frac{\partial c}{\partial \xi_i}=D\sum_{i=1}^{3}\frac{\partial^2 c}{\partial \xi_i^2} \tag{12}$$

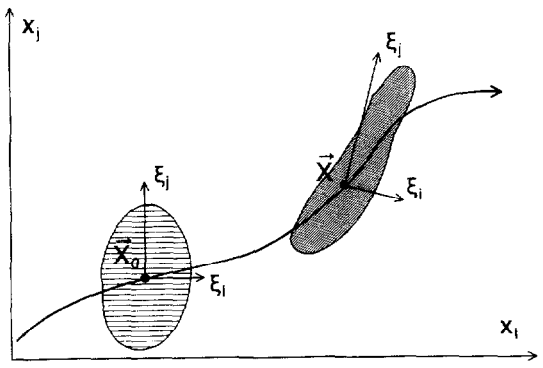

Fig. 2. A drop of tracer solution in an external flow field.

It is not necessary to solve this equation to characterize the shape of the spot. Following Tennekes and Lumley [20], and treating the concentration of the tracer substance as a three-dimensional probability density function, we can characterize the shape of the spot by concentration moments

$$I_{kl}=\frac{\int_{-\infty}^{+\infty}\int\int\int \xi_k\xi_l c(\vec{\xi},t)\,\mathrm{d}\xi_1\,\mathrm{d}\xi_2\,\mathrm{d}\xi_3}{\int_{-\infty}^{+\infty}\int\int\int c(\vec{\xi},t)\,\mathrm{d}\xi_1\,\mathrm{d}\xi_2\,\mathrm{d}\xi_3} \tag{13}$$

Such a definition allows the diagonal moment, I_{kk}, to be used as a quantity proportional to the square of the penetration distance, δ_k, of the tracer substance in the k direction (Fig. 3)

$$\delta_1^2:\delta_2^2:\delta a_3^2=I_{11}:I_{22}:I_{33} \tag{14}$$

and to estimate the spot volume

$$\frac{V(t)}{V(0)}\cong\sqrt{\prod_{k=1}^{3}\frac{I_{kk}(t)}{I_{kk}(0)}} \tag{15}$$

and the rate of growth of this volume

$$\frac{1}{V}\frac{\mathrm{d}V}{\mathrm{d}t}=\frac{1}{2}\sum_{k=1}^{3}\frac{1}{I_{kk}}\frac{\mathrm{d}I_{kk}}{\mathrm{d}t} \tag{16}$$

An expression describing the evolution in time of the concentration moments results from the integration of material balance (Eq. (12)) with the weight functions $\xi_k\cdot\xi_l$.

$$\frac{\mathrm{d}I_{kl}}{\mathrm{d}t}-\sum_{m=1}^{3}\left(\frac{\partial u_m}{\partial \xi_m}I_{kl}+\frac{\partial u_l}{\partial \xi_m}I_{km}+\frac{\partial u_k}{\partial \xi_m}I_{lm}\right)=2D\delta_{kl} \tag{17}$$

where δ_{kl} is the Kronecker delta

$$\delta_{kl}=\begin{cases}1 \text{ if } k=l\\ 0 \text{ if } k\neq l\end{cases} \tag{18}$$

For incompressible flows and $k=l$, Eq. (17) takes the form

$$\frac{\mathrm{d}I_{kk}}{\mathrm{d}t}-2\sum_{m=1}^{3}\frac{\partial u_k}{\partial \xi_m}I_{km}=2D \tag{19}$$

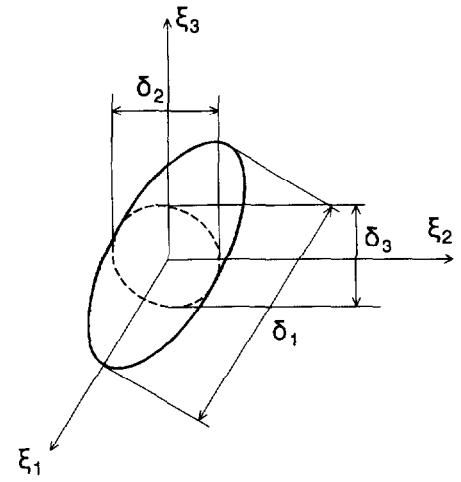

Fig. 3. Spatial characterization of a drop of tracer solution.

or

$$\frac{dI_{kk}}{dt}-2\sum_{m=1}^{3}(D_{km}+\Omega_{km})I_{km}=2D \tag{20}$$

where D_{km} and Ω_{km} are the components of the deformation and rotation tensors, respectively.

$$D_{km}=\frac{1}{2}\left(\frac{\partial u_k}{\partial \xi_m}+\frac{\partial u_m}{\partial \xi_k}\right) \tag{21}$$

$$\Omega_{km}=\frac{1}{2}\left(\frac{\partial u_k}{\partial \xi_m}-\frac{\partial u_m}{\partial \xi_k}\right). \tag{22}$$

Eq. (20) can be significantly simplified if it is possible to find a new local frame of reference (ξ_1', ξ_2', ξ_3') such that the off-diagonal moments vanish (i.e., $I_{km}'=0$ if $k\neq m$). This is possible when the considered spot has a symmetry plane, as in the case of a slab, sphere or ellipsoid. If the orientation of this plane is given by the unit vector, $\hat{\boldsymbol{n}}$, and one of the axes of the new local frame of reference (ξ_1', ξ_2', ξ_3'), e.g., k, is pointed in direction $\hat{\boldsymbol{n}}$ and the two other axes are parallel to the symmetry plane of the spot. Eq. (20) becomes

$$\frac{dI_{kk}'}{dt}-2D'_{kk}I_{kk}'=2D \tag{23}$$

On the other hand, the rotation transformation of the deformation tensor from the previous frame (ξ_1, ξ_2, ξ_3) to the new one (ξ_1', ξ_2', ξ_3') reads [21]

$$D_{kl}'=\sum_{i=1}^{3}\sum_{j=1}^{3}\cos\alpha_{ik}\cos\alpha_{jl}D_{ij} \tag{24}$$

where α_{ik} and α_{jl} are the angles between the old i and j axes and the new k and l axes, respectively. The assumption that the k axis is pointed in the same direction as $\hat{\boldsymbol{n}}$ enables Eq. (24) for $k=l$ to be rewritten in the more compact form

$$D_{kk}'=\tilde{D}:\hat{\boldsymbol{n}}\hat{\boldsymbol{n}} \tag{25}$$

Combining Eqs. (23) and (25) gives

$$\frac{1}{I_{kk}'}\frac{dI_{kk}'}{dt}=2\left[\tilde{D}:\hat{\boldsymbol{n}}\hat{\boldsymbol{n}}+\frac{D}{I_{kk}'}\right]=2\left[\frac{D}{I_{kk}'}-\alpha(\vec{X},t)\right] \tag{26}$$

where the second equality is obtained directly from Eq. (1), written for the incompressible flow. According to the last equation, the rate of change of the concentration moment depends on the rates of molecular diffusion and deformation, and thus is related to the characteristic times of diffusion and deformation.

$$t_D=I_{kk}'/D \tag{27}$$

$$t_F=\alpha^{-1} \tag{28}$$

In the case of laminae, and for $t_D\gg t_F$ the relation between the concentration moment, I_{kk}', and the lamina thickness, s, according to Eq. (13), reads

$$I_{kk}'=s^2/12 \tag{29}$$

Using this simplified assumption and expressing Eq. (26) in terms of s, we obtain the same relation as that derived previously by Ottino et al. [17], under the assumption that the kinematics of fluid motion dominates the process

$$\frac{1}{s}\frac{ds}{dt}=\tilde{D}:\hat{\boldsymbol{n}}\hat{\boldsymbol{n}}=-\alpha(\vec{X},t) \tag{30}$$

Hence, the concentration moments, as well as the striation thickness, can be used to characterize the process of micromixing. Furthermore, the rate of change of the concentration moments can also be related to the energetic efficiency of mixing using Eq. (6)

$$\frac{1}{I_{kk}'}\frac{dI_{kk}'}{dt}=2\left[\frac{D}{I_{kk}'}-\mathrm{eff}(\vec{X},t)\sqrt{\varepsilon/(2\mu)}\right] \tag{31}$$

Knowing the history of change of I_{kk}', it is easier to determine eff from Eq. (31) than from Eq. (6); to apply Eq. (6) directly, we need a complete knowledge of the fluid motion in time and space, including information on the orientation and distribution of all the interfaces in the system. Moreover, the description of mixing using the concentration moments is more general than that using the striation thickness because it includes the effects of molecular diffusion.

Introducing the time average of the deformation rate,

$$\langle\alpha(t)\rangle=\frac{1}{t}\int_0^t\alpha(\vec{X},t)dt'=\frac{1}{t}\int_0^t\mathrm{eff}(\vec{X},t')\sqrt{\varepsilon/(2\mu)}\,dt', \tag{32}$$

we can express the solution of Eq. (31) in the following form,

$$I_{kk}'(t)=[I_{kk}'(0)+2D\int_0^t e^{2\langle\alpha(t')\rangle t'}dt']e^{-2\langle\alpha(t)\rangle t} \tag{33}$$

Analysis of Eq. (33) shows that, when the spot of the tracer is contracted with a constant rate, $\langle\alpha\rangle=\alpha=\mathrm{const}>0$, in the direction perpendicular to its symmetry plane, the value of I_{kk}' and the associated penetration distance, δ_k', decrease and stabilize in time. When the spot is stretched with a constant rate in this direction, $\langle\alpha\rangle=\alpha=\mathrm{const}<0$, I_{kk}' and δ_k' increase exponentially in time. In the case of no deformation, the spot grows only due to molecular diffusion. The limiting solutions obtained in these three different cases are as follows

$$\delta_k'(t)\propto\sqrt{I_{kk}'(t)}$$

$$\cong\begin{cases}\sqrt{D/\alpha} & \text{if}\ \alpha>0 \ \text{and} \ t\gg\alpha^{-1}\\ \sqrt{2Dt} & \text{if}\ \alpha=0 \ \text{and} \ t\gg I_{kk}'(0)/D\\ \sqrt{I_{kk}'(0)-D/\alpha}\,e^{-\alpha t} & \text{if}\ \alpha<0 \ \text{and} \ t\gg-\alpha^{-1}\end{cases} \tag{34}$$

As pointed out by Ranz [16] and Ottino et al. [17], in the local frame of reference translating and rotating with a fluid

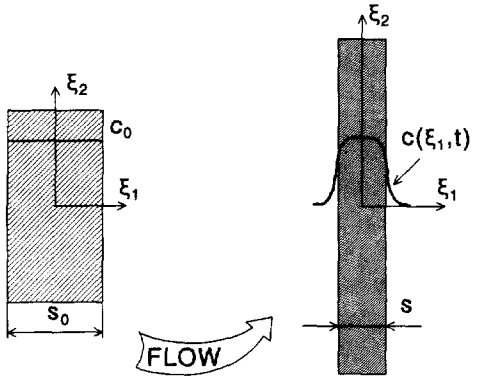

Fig. 4. Molecular diffusion of tracer substance outwards in a stretched slab.

element, the local flow tends to a two-dimensional stagnation flow

$$u_i=\alpha_i\xi_i, \text{ for } i=1, 2, 3 \text{ and } \alpha=-\alpha_1=\alpha_2,\ \alpha_3=0 \qquad (35)$$

Fig. 4 shows a slab containing a tracer solution deformed in such a flow. The tracer substance, initially distributed uniformly in the slab, diffuses outwards from the lamina into the surroundings; the molecular mass transfer in the directions parallel to the intermaterial surface is negligible, because for these directions $t_F \ll t_D$. Then the diagonal concentration moments become

$$I_{11}'(t)=\left[I_{11}'(0)-\frac{D}{\alpha}\right]e^{-2\alpha t}+\frac{D}{\alpha},$$

$$I_{22}'(t)=I_{22}'(0)\,e^{2\alpha t},\ I_{33}'(t)=I_{33}'(0) \qquad (36)$$

provided that $\langle\alpha\rangle=\alpha=\text{const}$. Introduction of the last results into Eqs. (15) and (16) gives the volume of the spot and its rate of growth

$$\frac{V(t)}{V(0)}=\left\{1+\frac{D}{\alpha I_{11}'(0)}\left[e^{2\alpha t}-1\right]\right\}^{0.5} \qquad (37)$$

$$\frac{1}{V}\frac{dV}{dt}=\left\{\frac{1}{\alpha}+\left[\frac{I_{11}'(0)}{D}-\frac{1}{\alpha}\right]e^{-2\alpha t}\right\}^{-1} \qquad (38)$$

When a very concentrated solution of one reactant is fed into a dilute solution of another reactant, the volume of the reaction zone is determined by the penetration distance of the highly concentrated substrate, and Eqs. (37) and (38) can be incorporated into the material balances of the reactants. Substrates remaining initially in the environment, depending on the relation between the rate of chemical reaction and the rate of micromixing, will either react instantaneously at the border of the expanding zone of the highly concentrated substrate or will be absorbed by this zone and react within it. In the first case, the reaction rate is directly proportional to the rate of increase of the volume occupied by the highly concentrated substrate. In the second case, the distribution of the less concentrated substrates inside the reaction zone can be assumed to be practically uniform when the zone expands more rapidly than the chemical reaction proceeds. In practice, we can compare the half reaction time and the time in which the volume of the reaction zone is doubled to find out which process is faster. For example, if the reaction zone has a shape of an elongated lamina of initial thickness, s_0, then, according to Eqs. (29) and (37), the volume of the reaction zone will be doubled in the time period equal to

$$t_V=\ln(1+0.25\alpha s_0^2/D)/(2\alpha) \qquad (39)$$

Eventually, for t_V smaller than the half reaction time, the concentrations of the reactants penetrating into the slab are almost uniformly distributed within the slab; this phenomenon simplifies, in many cases, the description of the chemical kinetics. In the case of a second-order reaction between A and C, as given by Eq. (43), the average rate of reaction within the slab can be expressed using the reactant concentrations averaged over the reaction zone.

In view of the above remarks, the material balance equation for reactant i can be written as follows

$$\frac{d}{dt}(Vc_i)=\frac{dV}{dt}<c_i>+VR_i \qquad (40)$$

where c_i is the mean concentration of this reactant in the reaction zone and $<c_i>$ is the environmental concentration of the same reactant. Rearrangement of Eq. (40) leads to

$$\frac{dc_i}{dt}=\frac{1}{V}\frac{dV}{dt}(<c_i>-c_i)+R_i \qquad (41)$$

This method is very similar to that used by Bałdyga and Bourne [22] in their model of turbulent micromixing. However, in the present case, the reaction zone enlarges not due to engulfment invoked by turbulent vorticity, but due to viscous deformation and molecular diffusion of the limiting reactant (Eq. (38)).

To illustrate the model application, let us consider a system of second-order, competitive, parallel reactions

$$A+B\xrightarrow{k_1}P_1 \text{ with } k_1\to\infty \qquad (42)$$

$$A+C\xrightarrow{k_2}P_2 \text{ and } R_i=-k_2c_Ac_C,\ i=A,C \qquad (43)$$

carried out in a semibatch reactor (Fig. 5). In this system, a concentrated solution of A is slowly fed into a premixture of B and C, while the chemically equivalent amounts of reactants are applied, i.e.,

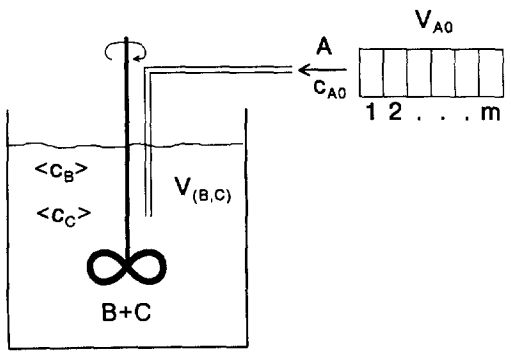

Fig. 5. Schematic representation of a semibatch addition of a solution of reactant A to a premixed solution of reactants B and C.

$$V_{A0}c_{A0}=V_{(B,C)0}c_{B0}=V_{(B,C)0}c_{C0}. \quad (44)$$

The final product distribution for the parallel reactions unequivocally depends on the course of mixing. For rapid mixing, the limiting substrate, A, is fully consumed in the first reaction with B. For slower mixing, A is also used up in the second reaction of finite rate (partially controlled by mixing). The history of mixing in such a system can be characterized by the final selectivity [22]

$$X=(N_{C0}-N_C)/N_{A0} \quad (45)$$

the value of which can vary from 0 (perfect mixedness) to 0.5 (complete segregation—both reactions controlled by mixing).

Slow addition of A-rich feed into the reactor (i.e., when the feed time is much longer than the macromixing time) ensures that there is no influence of macromixing on the product distribution. The semibatch operation can be simulated by discretizing the volume of A solution into m equal parts as shown in Fig. 5

$$V(0)=V_{A0}/m \quad (46)$$

and as performed by Bałdyga and Bourne [22]; in the present case, the effect of feed discretization on the final selectivity becomes negligible for $m \geq 100$. More over, in laminar mixing, for very slow feeding, the inlet stream is swept from the tip of the feeding pipe and subsequently forms a thin ribbon, elongated by the external flow.

The reactant dimensionless material balances, derived from Eqs. (38) and (41) for any elementary volume of A-rich solution become

$$\frac{dC_A}{d\Gamma}=-[(\theta_{II}-1)e^{-2\Gamma}+1]^{-1}(C_A+<C_B>)-\theta_I C_A C_C, \quad (47)$$

$$\frac{dC_C}{d\Gamma}=-[(\theta_{II}-1)e^{-2\Gamma}+1]^{-1}(C_C-<C_C>)-\theta_I C_A C_C \quad (48)$$

with the initial conditions

$$C_A(0)=1 \; C_C(0)=0 \quad (49)$$

where

$$\Gamma=\alpha t \quad (50)$$

and

$$C_i=c_i/c_{A0} \quad (51)$$

are the dimensionless time and reactant concentration, respectively. Relations between the characteristic times of molecular diffusion, ($t_D=I'_{11}(0)/D$), deformation, ($t_F=\alpha^{-1}$), and reaction ($t_R=1/(k_2c_{A0})$) appear in Eqs. (47) and (48) in the form of the dimensionless parameters

$$\theta_I=\frac{t_F}{t_R}=\frac{k_2c_{A0}}{\alpha} \quad (52)$$

$$\theta_{II}=\frac{t_D}{t_F}=\frac{\alpha I_{11}'(0)}{D} \quad (53)$$

Eqs. (47) and (48) should be integrated for each elementary volume of the feed until the limiting substrate A has been fully consumed.

The initial composition of the environment is

$$<C_A>_0=0, \; <C_B>_0=F_B/a, \; <C_C>_0=F_C/a \quad (54)$$

where

$$F_i=N_{i0}/N_{A0} \quad (55)$$

and

$$a=V_{(B,C)0}/V_{A0} \quad (56)$$

are the initial stoichiometric and volume ratios, respectively. The values of $<C_B>$ and $<C_C>$ decrease due to chemical reaction and dilution. Therefore if the k part of the feed ($1 \leq k \leq m$) has reacted in time Γ_k, by using Eq. (37), we can find the composition of the surroundings of the $k+1$ part as follows

$$<C_B>_k=<C_B>_{k-1}\times\left[1-(ma+k)^{-1}\left(1+\frac{e^{2\Gamma_k}-1}{\theta_{II}}\right)^{0.5}\right] \quad (57)$$

$$<C_C>_k=<C_C>_{k-1}+[C_C(\Gamma_k)-<C_C>_{k-1}](ma+k)^{-1}\left(1+\frac{e^{2\Gamma_k}-1}{\theta_{II}}\right)^{0.5} \quad (58)$$

Hence, the final selectivity of Eqs. (42) and (43) depends on five dimensionless parameters

$$X=f(\theta_I,\theta_{II},a,F_B,F_C) \quad (59)$$

To enable a direct comparison to be made of the results obtained for different volume ratios of reactant solutions, but for the same number of reactant moles, it is convenient to replace θ_I with a new dimensionless parameter referring to the average initial concentration of substrate A [22]

$$\bar{\theta}_I=\frac{k_2\bar{c}_{A0}}{\alpha}=\frac{k_2c_{A0}}{\alpha(a+1)}=\frac{\theta_I}{a+1} \quad (60)$$

Fig. 6 presents the effect of the time constant ratio, θ_{II}, and the volume ratio, a, on the final selectivity, X, predicted by the model for $\bar{\theta}_I=0.1$. The time constant ratio, θ_{II}, is proportional to the initial value of the concentration moment and consequently to the square of the penetration distance ($\theta_{II} \sim \delta_I'^2(0)$); therefore, for $\alpha/D=$ const, Fig. 6 shows how the initial size of the spot influences the product distribution. As can be seen, there is a region of θ_{II} where X is strongly dependent on $\delta_I'(0)$. In this region the characteristic diffusion time is from $1–10^4$ times lower than the characteristic deformation time and, therefore, $\delta_I'(0) < (Dt_F)^{0.5}$). For

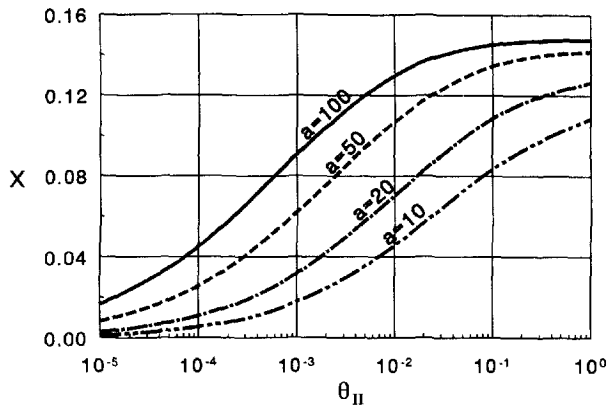

Fig. 6. Effect of the time ratio, θ_{II}, and the volume ratio, a, on the selectivity, X; $F_B = F_C = 1$, $\bar{\theta}_I = 0.1$.

either rapid diffusional mixing (proceeding when $\delta_1'(0) \ll (Dt_F)^{0.5}$) or very slow diffusional mixing (taking place when $\delta_1'(0) > (Dt_F)^{0.5}$) the initial size of the spot has little effect on the final selectivity. Fig. 6 also shows that the selectivity, X, is much less sensitive to the volume ratio, a, in these two extreme cases than when $10^{-4} < \theta_{II} < 1$. It should be noted that decreasing the volume ratio, but keeping the same amounts of reactants always improves mixing, because it takes less time for reagent A to be fully consumed; the shorter the mixing time the smaller the chance for the slower reaction to proceed and increase the selectivity.

To determine the effect of the deformation rate alone on the final selectivity, it is convenient to introduce a new dimensionless parameter which is the product of $\bar{\theta}_I$ and θ_{II}.

$$\bar{\theta}_{III} = \bar{\theta}_I \theta_{II} = \frac{1}{1+a}\frac{t_D}{t_R} = \frac{k_2 c_{A0} I_{11}'(0)}{(1+a)D} \tag{61}$$

Fig. 7 illustrates the influence of θ_{II} on the selectivity, X, for four values of $\bar{\theta}_{III}$. As expected, increasing θ_{II}, which for $\bar{\theta}_{III} = const$ and $I_{11}'(0)/D = \text{const}$ is equivalent to faster convectional mixing ($\theta_{II} \sim \alpha$), always decreases the selectivity. On the other hand, increasing $\bar{\theta}_{III}$ increases the selectivity due to the decrease in the characteristic reaction time, t_R.

The computations have been performed for $\bar{\theta}_I$, θ_{II} and $\bar{\theta}_{III}$ satisfying the criterion

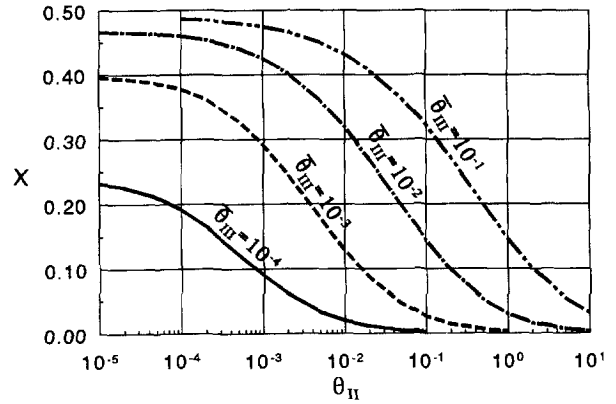

Fig. 7. Effect of the time ratios θ_{II} and $\bar{\theta}_{III}$ on the selectivity, X; $F_B = F_C = 1$, $a = 100$.

$$\frac{\bar{\theta}_I}{2}\ln(1+3\theta_{II}) = \frac{\bar{\theta}_{III}}{2\theta_{II}}\ln(1+3\theta_{II}) < 1 \tag{62}$$

which ensures that the time period of doubling the reaction zone volume is smaller than the half reaction time of the slower reaction and hence enables the micromixing model to be employed.

3. Experimental details

The chemical reactions employed to investigate micromixing experimentally were the neutralization reaction of sodium hydroxide (A) by hydrochloric acid (B) and the alkaline hydrolysis of ethyl chloroacetate (C), i.e., the system used previously in studies of turbulent micromixing [23,24]

$$NaOH + HCl \xrightarrow{k_1} NaCl + H_2O \tag{63}$$

$$NaOH + CH_2ClCOOC_2H_5 \xrightarrow{k_2} CH_2ClCOONa + C_2H_5OH \tag{64}$$

At $T = 298.15$ K, we have $k_1 \approx 10^{11}$ dm^3 mol^{-1} s [25] and $k_2 = 33.2$ dm^3 mol^{-1} s [26]. The characteristic reaction time

$$t_{R_i} = 1/(k_i c_0) \quad (i = 1,2) \tag{65}$$

for neutralization equals $t_{R1} = 10^{-9}$ s and for hydrolysis equals $t_{R2} = 3$ s, when $c_0 = 0.01$ mol dm^{-3}. On the other hand, the micromixing time defined by Bałdyga and Bourne [10]

$$t_M = \text{arcsinh}(0.76\alpha s_0^2/D)/(2\alpha) \tag{66}$$

and calculated for typical values of the deformation rate ($\alpha = 1$ s^{-1}), molecular diffusivity ($D = 10^{-10}$ m^2 s) and striation thickness ($s_0 = 10^{-4}$ m), characteristic for the process of laminar mixing, equals 2.5 s.

Comparison of t_{R1}, t_{R2} and t_M shows that the neutralization reaction is completely controlled by mixing (instantaneous), whereas the hydrolysis reaction is sufficiently fast to compete with mixing. Therefore the product distributions of these reactions, carried out in an unpremixed feed system, should be strongly related to the history of mixing on the molecular scale.

Polyethylenepolypropylene glycol (trade name Breox 75 W 18000) was applied to increase the viscosity of the aqueous solutions in which the test reactions were carried out. Using this polymer allows the viscosity of water to be increased more than 20 000 times (Fig. 8) while preserving the Newtonian character of the resulting solution [27]. The polymer is chemically stable at room temperature and in dilute solutions of the reagents tested. Increasing the HCl concentration above 1 mol dm^{-3} results in a rapid fall in the solution viscosity, whereas concentrations of NaOH which are too high result in the formation of a colloidal solution (Fig. 9) [27].

The viscosity-increasing polymer decreases the molecular diffusivities of all the reactants. Fig. 10 shows the variation

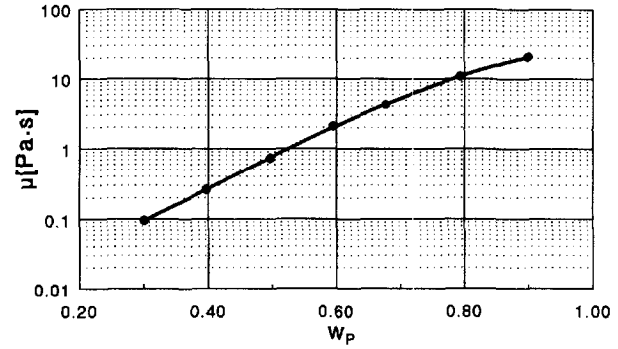

Fig. 8. Viscosity of aqueous solutions of polyethylenepolypropylene glycol at 298.1 K.

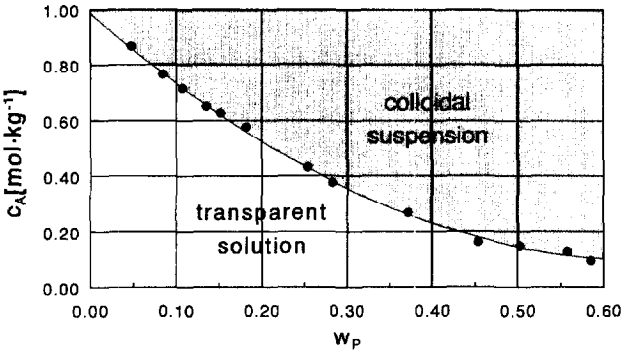

Fig. 9. Limiting NaOH concentrations in aqueous solutions of polyethylenepolypropylene glycol at 298.1 K.

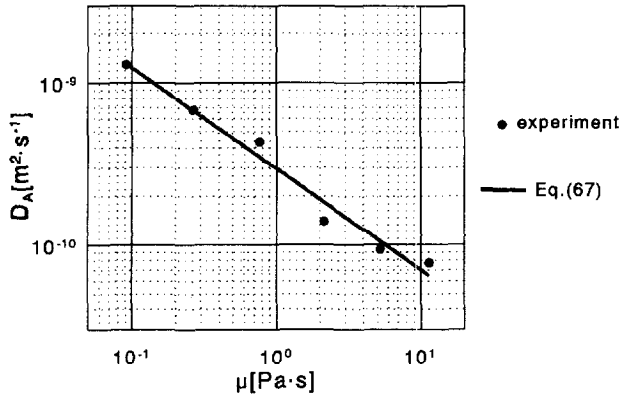

Fig. 10. Variation of the molecular diffusivity of NaOH as a function of the viscosity of aqueous solutions of polyethylenepolypropylene glycol at 298.1 K.

of the NaOH diffusivity coefficient as a function of the solution viscosity at $T=298.15$ K. The diffusivity coefficient was determined experimentally by measuring the amount of NaOH which diffused from one half of a small cylindrical cell (diameter, 2 cm; length, 8 cm) to the other half of the cell after a specified period of time. The experimentally determined correlations for the coefficients of molecular diffusivity of NaOH, HCl and $CH_2ClCOOC_2H_5$ in a solution of polyethylenepolypropylene glycol are as follows [27]

$$D_A = 2.97\times10^{-10}/\mu^{0.622} \quad (67)$$

$$D_B = 8.48\times10^{-10}/\mu^{0.238} \quad (68)$$

$$D_C = 0.609\times10^{-10}/\mu^{0.649} \quad (69)$$

A conductimetric method was employed to measure the rate constant of the ester hydrolysis carried out in a batch reactor working in the kinetic regime. These experiments showed practically no change in k_2 for a mass fraction of the polymer varying from 0 to 0.4 [27].

Experimental investigations of micromixing with parallel reactions of Eqs. (63) and (64) were conducted at $T=298.15$ K in two reactors of different geometry and operational mode. The first reactor was a glass tank 0.096 m in diameter, fitted with four baffles and a four-bladed, pumping-downwards, pitched-blade turbine as shown in Fig. 11. The turbine blades were 1 mm thick and inclined 45° from the vertical. The turbine, its shaft and the blades were made of stainless steel. The reactor, initially containing a premixed, dilute solution of HCl and $CH_2ClCOOC_2H_5$, was fed with a concentrated solution of NaOH by means of a syringe pump through a small glass pipe with an internal diameter of 1.6 mm. The orifice of the dosing pipe was placed above the rotating turbine. The viscosities of the mixed solutions were increased to 0.3 Pa s with polyethylenepolypropylene glycol to reduce the turbine Reynolds number and thus to obtain a laminar flow regime in the tank. The solution densities were equalized by the addition of KCl to the solution of acid and ester in order to avoid gravitational separation.

High pressure liquid chromatography was employed to determine the final concentration of ethyl chloroacetate in the resulting mixtures. The chromatographic analysis was carried out on a Waters Nova-Pak C-18 column (length, 15 cm; diameter, 3.9 mm), with an eluent composed of water and acetonitrile (H_2O–CH_3CN, 60 40), and ethyl acetate as internal standard. The composition of the eluted solution was analyzed by a Waters UV absorbance detector (type 486), tuned to a wavelength of 220 nm.

The second reactor was a Werner and Pfleiderer ZSK 25 twin-screw extruder fed continuously with two reactant solutions (Fig. 12) of viscosity 0.28 Pa s, containing poly-

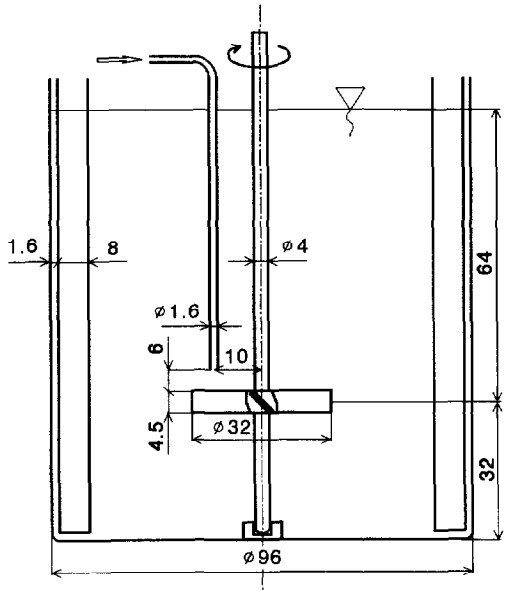

Fig. 11. Diagram of a semibatch reactor.

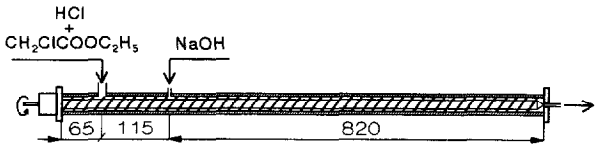

Fig. 12. Diagram of a twin-screw extruder.

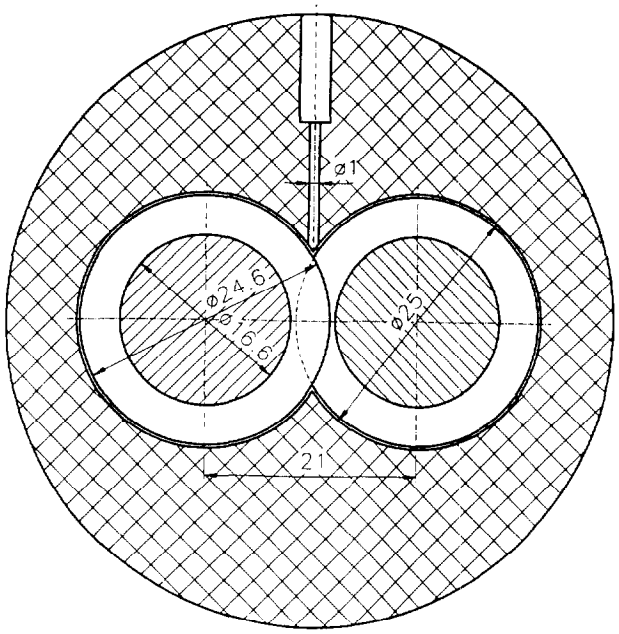

Fig. 13. Cross-sectional view of a twin-screw extruder.

ethylenepolypropylene glycol. The extruder screws were double-flighted, co-rotating, self-wiping and partially intermeshing. The screw helix angle was 25.5° and the flight and channel widths were 13.1 mm and 3.8 mm, respectively. The extruder was completely filled with the mixed liquids and worked with an open discharge. The solution of HCl and $CH_2ClCOOC_2H_5$ was supplied to the main feed throat and then conveyed by the screws along the extruder. The solution of NaOH was fed centrally into the extruder channel (Fig. 13) via a syringe pump. Samples of the resulting mixture were taken after the processing conditions became stable and were analyzed chromatographically.

4. Results and discussion

The results of the preliminary model calculations, presented in Fig. 6, indicate that the final selectivity of the parallel reactions, carried out in the semibatch reactor, can be strongly influenced by the initial scale of the feeding stream. Hence, the aim of the first tests performed in the semibatch reactor was to detect this effect and to provide data to identify the model parameters. In these experiments, all the process conditions were kept unchanged, except for the feeding rate of the NaOH solution, which ranged from 0.18 to 2 cm^3 min^{-1}. As a result, a strong influence of the feeding time on the selectivity was determined as shown in Fig. 14. Visual observations of the feeding stream coloured with phenol-

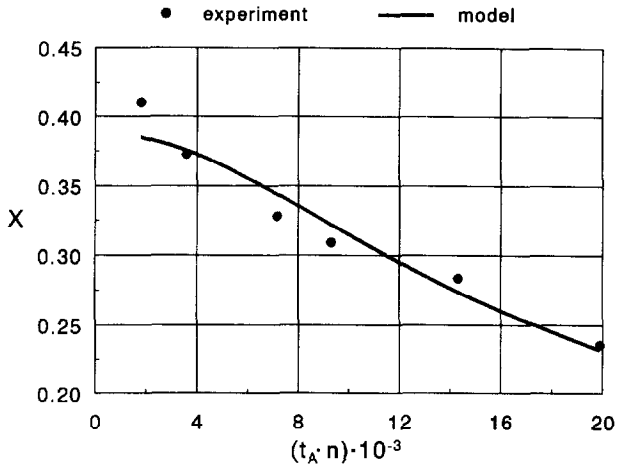

Fig. 14. Measured and calculated values of the selectivity, X, for the semibatch reactor; effect of the feeding time, t_A, (first series of experiments).

phthalein showed that it had a thin ribbon shape; it was swept from the tip of the feeding pipe, carried downward's to the turbine along a spiral trajectory and then conveyed away in the radial direction. The ribbon thickness, s_0, can be related to the feeding rate, Q_A, and consequently to the feeding time, t_A, by means of the continuity equation.

$$Q_A = V_{A0}/t_A = s_0 b v \tag{70}$$

The initial ribbon width, b, should be close to the diameter of the feeding pipe (1.6 mm), whereas the local fluid velocity, v, should be correlated with the speed of the turbine blades

$$v = \psi n d \tag{71}$$

where ψ is the dimensionless function of the system geometry and Reynolds number, Re.

Considering the fact that the liquid depth in the reactor was equal to the reactor diameter after putting in half of the NaOH solution, we have

$$V_{A0} = (\pi/D_T^2 H)/(4a+2) \tag{72}$$

A combination of Eqs. (29), (56,) (70)–(72) allows the initial value of the concentration moment associated with the feeding stream to be related to the process parameters

$$\frac{I_{11}'(0)}{d^2} = \frac{s_0^2}{12d^2} = \frac{(13.5\pi)^2}{12}\left(\frac{d}{b}\right)^2 \frac{1}{(2a+1)^2\psi^2(t_A n)} \tag{73}$$

The constant value of the deformation rate, $\langle\langle\alpha\rangle\rangle$, was used in the model computations for each set of process conditions. This assumed constant rate of deformation can be interpreted as the value averaged over both the lifetime of the limiting reactant (NaOH) and the feeding time of the NaOH solution. According to Eq. (6), the deformation rate at any material point in the system depends on the energetic efficiency of mixing, the viscosity of the liquid and the local rate of energy dissipation per unit volume. Hence the averaging procedure used for the rate of deformation must also be applied for the energetic efficiency of mixing and the local rate of energy dissipation per unit volume.

$$\langle\langle \text{eff}\,\varphi^{0.5}\rangle\rangle = \langle\langle\alpha\rangle\rangle / \sqrt{\langle\varepsilon\rangle_V/(2\mu)} \tag{74}$$

where φ denotes the ratio of the local value of the rate of energy dissipation to the mean power input per unit volume in the mixer

$$\varphi = \varepsilon/\langle\varepsilon\rangle_V \tag{75}$$

Eq. (74) defines a practical efficiency $\langle\langle \text{eff}\varphi^{0.5}\rangle\rangle$ which combines both the theoretical efficiency of mixing and the distribution of the rate of energy dissipation within the system.

The mean rate of energy dissipation per unit volume, $\langle\varepsilon\rangle_V$, for the cylindrical tank reactor can be calculated from

$$\langle\varepsilon\rangle_V = (4P)/(\pi H D_T^2) \tag{76}$$

The total power input, P, can be estimated using the experimental correlation for the power number, Po.[1]

$$\log_{10}\text{Po} = 1.687 - 1.080\log_{10}\text{Re} + 0.185(\log_{10}\text{Re})^2 \tag{77}$$

which is valid for $1 < \text{Re} < 740$. Combining Eqs. (74) and (76) yields

$$\frac{\langle\langle\alpha\rangle\rangle d^2\rho}{\mu} = \frac{\langle\langle \text{eff}\,\varphi^{0.5}\rangle\rangle}{(13.5\pi)^{0.5}}\text{Po}^{0.5}\,\text{Re}^{1.5} \tag{78}$$

Using Eqs. (73) and (78), we can express the two time ratios $\bar{\theta}_I$ and θ_{II} (Eqs. (60) and (53)) as follows

$$\bar{\theta}_I = \frac{(13.5\pi)^{0.5}}{\langle\langle \text{eff}\varphi^{0.5}\rangle\rangle}\frac{\overline{\text{Da}}}{\text{ScPo}^{0.5}\text{Re}^{1.5}} \tag{79}$$

$$\theta_{II} = \frac{(13.5\pi)^{1.5}}{12}\left(\frac{d}{b}\right)^2\frac{\langle\langle \text{eff}\varphi^{0.5}\rangle\rangle}{\psi^2(t_A n)^2}\frac{\text{Sc}\,\text{Re}^{1.5}\,\text{Po}^{0.5}}{(2a+1)^2} \tag{80}$$

In the considered case we have $a = 19$, $F_B = F_C = 1$, $\text{Re} = 6.08$, $\text{Sc} = 4.47\times10^5$, $\overline{\text{Da}} = 5.41\times10^5$ and $d/b = 20$. Unknown a priori values of $\langle\langle \text{eff}\varphi^{0.5}\rangle\rangle$ and ψ were determined by fitting (least-squares method) the computed selectivities to the experimental points shown in Fig. 14. The best fit was achieved for $\psi = 4.25$ and $\langle\langle \text{eff}\varphi^{0.5}\rangle\rangle = 0.05$. A comparison of the theoretical curve with the experimental points (Fig. 14) shows that the agreement is very good, except for one point obtained for the shortest feeding time. The initial values of the ribbon thickness calculated from Eq. (73) were in the range 0.008–0.092 mm, which proves that the feeding stream was initially subjected to rapid deformation. The high efficiency obtained in the computations shows that the reaction zone must have been localized near the agitator. In this area, the local rates of energy dissipation per unit volume should considerably exceed the average in the whole reactor ($\varphi = \varepsilon/\langle\varepsilon\rangle_V > 1$).

In the second series of experiments, the feeding time was kept constant, while the rotational frequency of the turbine was varied. As a result, a very strong effect of the Reynolds number on the final selectivity was found (Fig. 15). These experimental data were subsequently used to determine the correlation between the dimensionless parameter ψ and the Reynolds number. It was assumed that

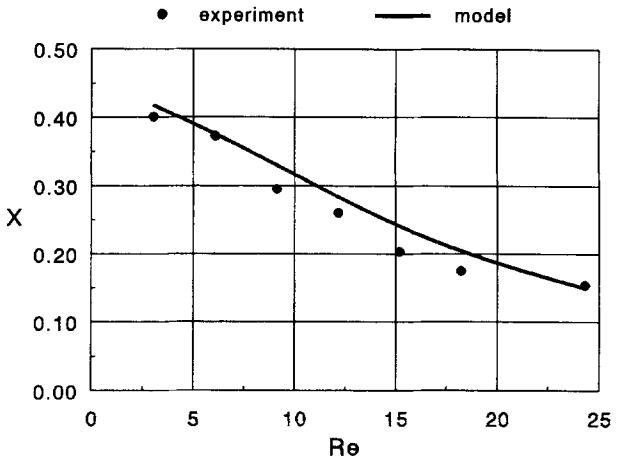

Fig. 15. Measured and calculated values of the selectivity, X, for the semi-batch reactor; effect of the Reynolds number, Re (second series of experiments).

$$\psi(\text{Re}) = 4.25\left(\frac{\text{Re}}{6.08}\right)^{\gamma} \tag{81}$$

Moreover, to simplify the calculation of θ_{II} Eq. (80) was modified

$$\theta_{II} = \frac{(13.5\pi)^{1.5}}{12}\left(\frac{d}{b}\right)^2\frac{\langle\langle \text{eff}\,\varphi^{0.5}\rangle\rangle}{\text{Sc}(2a+1)^2}\left(\frac{d^2}{Dt_A}\right)^2\frac{1}{\psi^2}\left(\frac{\text{Po}}{\text{Re}}\right)^{0.5} \tag{82}$$

where $d^2/(Dt_A) = 759.3$. Comparing the calculated selectivity with the selectivity determined experimentally at $\text{Re} = 24.27$, the value $\gamma = 0.5$ was estimated and Eq. (81) finally became

$$\psi(\text{Re}) = 1.73\text{Re}^{0.5} \tag{83}$$

Only in the creeping flow regime and for well-developed turbulent flow, should we expect ψ to be independent of Re. In our case, laminar flow with some inertial effects is considered, so some influence of the Reynolds number on the flow pattern should exist. Several examples of such an influence on the experimentally measured mixing times, and therefore on the flow patterns, in stirred tank reactors for $10 < \text{Re} < 100$ are given by Hoogendoorn and Hartog [7] and Nagata [8]. Fig. 15 shows that the agreement between the model predictions and the experimental points is satisfactory when Eq. (83) is used.

The identification of the model parameters enables the effect of other process conditions on the final selectivity to be predicted. Figs. 16 and 17 present a comparison between the experimentally determined and calculated effect of varying the initial volume ratio on the final selectivity for two different values of the Reynolds number. The model correctly predict's the effect of the volume ratio on the selectivity.

The combined effects of the feeding rate and the revolution frequency of the screws on the final selectivity were investi-

[1] L. Smit, DSM Research, Geleen, The Netherlands, personal information.

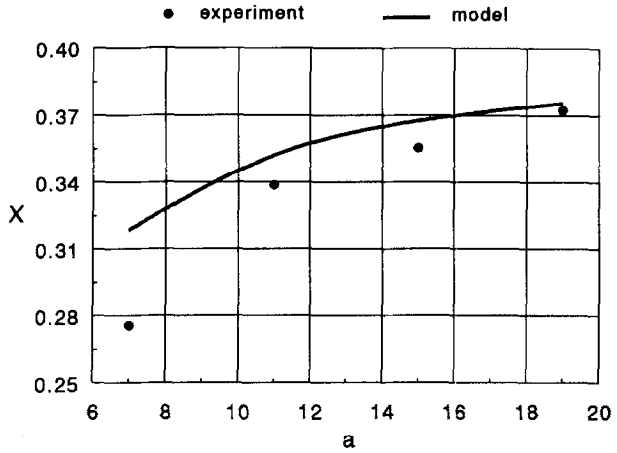

Fig. 16. Measured and calculated values of the selectivity, X, for the semi-batch reactor; effect of the volume ratio, a (third series of experiments, Re = 6.08).

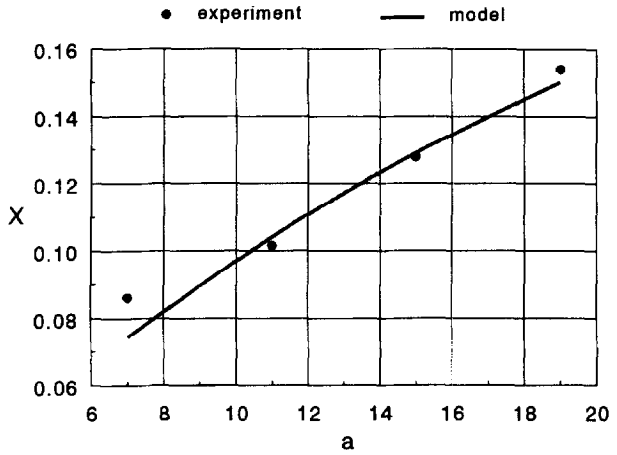

Fig. 17. Measured and calculated values of the selectivity, X, for the semi-batch reactor; effect of the volume ratio, a (fourth series of experiments, Re = 24.27).

gated in the extruder. In each series of tests, conducted for three different values of the volume ratio of the reactant solutions, the discharge rate, Q, was found to be a linear function of the revolution frequency, n

$$Q = Q_A + Q_{B,C} = (1+a)Q_A = q(n - n_b) \tag{84}$$

where n_b denotes the minimum revolution frequency of the screws required to overcome a hydrostatic back-pressure, caused by positioning the outlet of the extruder discharge pipe 30 cm above the liquid level in the extruder inlet throat. For each experimental point, the revolution frequency of the screws was measured by an electronic counter, whereas the total extruder throughput was determined by weighing the outflowing liquid, collected during a specified period of time. A least-squares method was applied to determine the values of q and n_b for each series of tests independently. Visual observations of the iodine coloured stream injected into the extruder channel (in the same way as the NaOH solution in the subsequent experiments with the test reactions) showed that the fed stream was wiped by the screw flights from the inlet orifice. The wiped stream had a thin ribbon shape, elongated and mixed with the bulk flow. Thus, assuming that the local fluid velocity, v, is directly proportional to the revolution frequency of the screws and combining continuity equation, Eq. (70) with Eq. (84), we can find the initial thickness of the NaOH stream from

$$s_0 = \frac{Q_A}{bv} = \frac{q}{(1+a)\psi_E b d_E}\left(1 - \frac{n_b}{n}\right) \tag{85}$$

where ψ_E is the dimensionless constant depending on the system geometry. As a result, the initial value of the concentration moment associated with the feeding stream reads

$$\frac{I(0)}{d_E^2} = \frac{1}{12(1+a)^2\psi_E^2}\left(\frac{d_E}{b}\right)^2\left(\frac{q}{d_E^3}\right)^2\left(1 - \frac{Re_{Eb}}{Re_E}\right)^2 \tag{86}$$

The power transferred from the screw shafts to the liquid in the extruder produces drag and pressure flow of the liquid in the extruder and the discharge pipe. Therefore, the power dissipated in the extruder due to viscous deformation is equal to the difference between the total power input and the power required to overcome a flow resistance outside the extruder. The total power input was calculated from a correlation developed by Denson and Hwang [28]. Hence, the average rate of energy dissipation per unit volume in the extruder reads

$$\langle \varepsilon \rangle_V = 3.9 \times 10^3\, \mu n^2 + 1.4 \times 10^{-2}\, n\Delta p - 4.1 \times 10^{-2}\frac{q}{d_E^3}(n - n_b)\Delta p \tag{87}$$

where Δp is the overpressure developed in the extruder. After combining Eqs. (32), (75) and (87) we obtain an expression for the rate of deformation of the liquid elements averaged over the lifetime of the limiting reactant (NaOH) in the extruder

$$\frac{\langle \alpha \rangle d_E^2 \rho}{\mu} = \langle eff\varphi^{0.5} \rangle \times \left\{1.95 \times 10^3 Re_E^2 + \left[7 \times 10^{-3}\, Re_E - 2.05 \times 10^{-2} \times \left(\frac{q}{d_E^3}\right)(Re_E - Re_{Eb})\right]\frac{\Delta p d_E^2 \rho}{\mu^2}\right\}^{0.5} \tag{88}$$

It should be noted that, as in the case of the semibatch tank reactor, the energetic efficiency of mixing is related to the mean rate of energy dissipation per unit volume of the mixer. From the initial value of the concentration moment and the average rate of deformation related to the process conditions, we can express the time ratios $\bar{\theta}_I$ and θ_{II} (Eqs. (60) and (53)) in the following way

$$\bar{\theta}_I = \frac{\overline{Da}_E}{Sc}\left(\frac{\langle \alpha \rangle d_E^2 \rho}{\mu}\right)^{-1} \tag{89}$$

$$\theta_{II} = \frac{Sc}{12\,\psi_E^2(1+a)^2}\left(\frac{d_E}{b}\right)^2\left(\frac{q}{d_E^2}\right)^2\left(1 - \frac{Re_{Eb}}{Re_E}\right)^2 \langle \alpha \rangle d_E^2 \frac{\rho}{\mu} \tag{90}$$

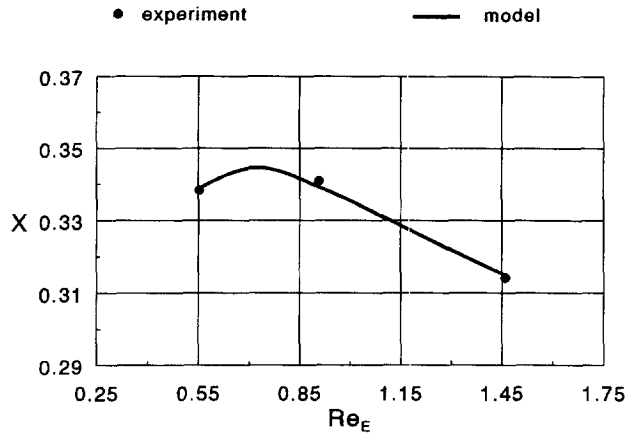

Fig. 18. Measured and calculated values of the selectivity, X, for the twin-screw extruder; effect of the Reynolds number, Re_E (first series of experiments).

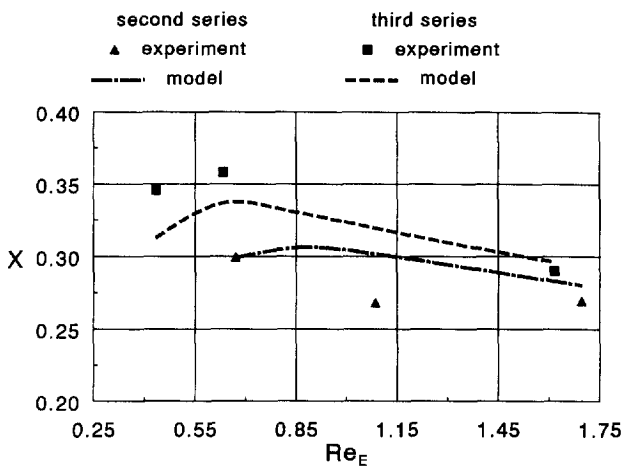

Fig. 19. Measured and calculated values of the selectivity, X, for the twin-screw extruder; effect of the Reynolds number, Re_E, and the volume ratio, a (second and third series of experiments).

As for the first reactor, $\langle \mathrm{eff}\varphi^{0.5}\rangle$ and ψ_E were determined by fitting the computed selectivities to the results of the experiments. Due to the stationary mode of the extruder operation and the small volume fraction of the reaction zone, the composition of the environment of the reaction zone was given by Eq. (54) along the reactor.

Fig. 18 shows the results of the first series of experiments with test reactions of Eqs. (63) and (64) conducted in the extruder ($a=14.9$, $F_B=0.881$, $F_C=0.993$, $Sc=4.03\times10^5$, $\overline{Da}_E=3.12\times10^5$, $d_E/b=25$, $q/d_E^3=0.135$, $Re_{Eb}=0.279$) and the results of modelling. In this case, the best fit was achieved for $\langle \mathrm{eff}\varphi^{0.5}\rangle=0.0075$ and $\psi_E=69.1$. The low value of the efficiency determined in the computations is caused by the very high energy dissipation in the drag flow occurring between the tips of the screw flights and the extruder barrel, which is accompanied by very poor growth of the intermaterial surface area. The predominance of drag flow in this area of the extruder channel was also the main reason why the dimensionless parameter, ψ_E, did not depend on the Reynolds number, Re_E. It should also be stressed that both the experiment and theory indicate that there is a maximum selectivity for small Reynolds numbers. To explain this phenomenon, it should be noted that, according to Eq. (85), for a revolution frequency slightly higher than n_b, a small increase in n results in a large increase in the initial thickness of the feeding stream, s_0, and also increases the characteristic diffusion time, t_D, which is proportional to the square of s_0. When the revolution frequency increases, s_0 and t_D stabilize and approach their upper limits. On the other hand, the characteristic deformation time, $t_F=1/\langle\alpha\rangle$, is inversely proportional to the revolution frequency in the laminar flow regime as given by Eq. (88). Hence, increasing the revolution frequency of the screws, decreases the rate of diffusional mixing and, at the same time, increases the rate of convectional mixing. For Reynolds numbers close to Re_{Eb}, the first effect is more important and the selectivity increases with increasing Re_E, whereas, for large Reynolds numbers, the second effect prevails and the selectivity decreases with increasing Re_E. Thus the maximum selectivity is observed for the intermediate values of Re_E.

Fig. 19 shows the results of the second ($a=18.1$, $F_B=0.958$, $F_C=0.915$, $Sc=4.03\times10^5$, $\overline{Da}_E=3.25\times10^5$, $d_E/b=25$, $q/d_E^3=0.143$, $Re_{Eb}=0.367$) and third ($a=23.7$, $F_B=1.024$, $F_C=1.007$, $Sc=4.03\times10^5$, $\overline{Da}_E=3.01\times10^5$, $d_E/b=25$, $q/d_E^3=0.189$, $Re_{Eb}=0.285$) series of experiments carried out in the extruder compared with the results of the computations conducted using the earlier determined values of $\langle \mathrm{eff}\varphi^{0.5}\rangle$ and ψ_E. It can be seen that the model account's sufficiently well for the influence of the Reynolds number, initial volume ratio and other process parameters on the selectivity of the parallel reactions.

5. Conclusions

Laminar micromixing has been described as the process of generation of an intermaterial area between the fluids being mixed, accompanied by molecular diffusion and chemical reactions proceeding within the deformed fluid striations. Little attention has been paid to the processes of mass exchange between the lamellar structures and their surroundings, or to the influence of local flow conditions on the initial distribution of the material in these structures. Despite these simplifications, the models available in the literature usually require complicated methods of solution of the material balance equations, which makes them difficult to apply in practice. Finally, there is a lack of a good reactive tracer method for the experimental investigation of the process of laminar micromixing and for the provision of sufficient data for the determination of the energetic efficiency of mixing in the system.

In the present work, a new model of laminar micromixing was developed by applying an integral transformation to a material balance equation in the Lagrangian frame of reference. The transformed equation was expressed in terms of integral concentration moments, which, in contrast with

quantities such as the striation thickness and intermaterial surface area, characterize not only convectional mixing but also mixing on the molecular scale. The proposed model correctly describes the mixing of a small volume of highly concentrated solution of one reactant with a large volume of a dilute solution of another reactant. The model predicts the effects of the initial stoichiometric ratio of the reactants, the volume ratio of the mixed solutions, the feeding rate of the mixed solutions, the flow conditions and the reaction kinetics on the selectivity of complex reactions.

A system of competitive, parallel reactions and a viscosity-increasing agent were used to study experimentally micromixing in laminar flow. The method was applied to two systems: a semibatch tank reactor and an on-line reactor (twin-screw extruder). The influence of processing conditions, such as the feeding time, the revolution frequency of the mixing elements and the volume ratio of the mixed solutions, on the selectivity of the test reactions was determined.

The experimental results were successfully interpreted by the proposed micromixing model. The model can be used to determine the energetic efficiency of mixing related to the mean rate of energy dissipation per unit volume in the mixer ($\langle\langle \mathrm{eff}\varphi^{0.5}\rangle\rangle = 5\%$ in the semibatch reactor and $\langle \mathrm{eff}\varphi^{0.5}\rangle = 0.75\%$ in the twin-screw extruder) and other parameters characterizing the investigated system, based on the results of the experiments with parallel reactions. This procedure can be applied to any system where micromixing is of importance, and thus allows a direct and strict comparison of systems differing in geometry and/or mode of operation.

Acknowledgements

This work was financially supported by DSM Research, Geleen, The Netherlands.

Appendix A. Nomenclature

A, B, C	Substrates
a	Volume ratio of reactant solutions defined by Eq. (56)
a_V	Intermaterial area per unit volume (m^{-1})
b	Width of a feeding stream (m)
C_i	Dimensionless concentration of reactant i defined by Eq. (51)
c	Concentration of tracer substance (mol m^{-3})
c_i	Concentration of reactant i (mol m^{-3})
D	Molecular diffusivity of tracer substance (m^2 s^{-1})
D_T	Tank reactor diameter ($3d$) (m)
D_i	Molecular diffusivity of reactant i (m^2 s^{-1})
D_{ij}	Component of deformation tensor (s^{-1})
$\vec{\vec{D}}$	Deformation tensor (s^{-1})
$\overline{\mathrm{Da}}$	Damköhler number for tank reactor ($k_2 c_{A0} d^2 D_A^{-1}(1+a)^{-1}$)
$\overline{\mathrm{Da}}_E$	Damköhler number for extruder ($k_2 c_{A0} d_E^2 D_A^{-1}(1+a)^{-1}$)
d	Agitator diameter (m)
d_E	Extruder barrel diameter (m)
eff	Energetic efficiency of mixing defined by Eq. (6)
F_i	Stoichiometric ratio defined by Eq. (55)
H	Liquid depth in tank reactor ($\cong 3d$) (m)
I_{kl}	Concentration moment defined by Eq. (13) (m^2)
k, k_i	Second order reaction rate constants (m^3 mol^{-1} s^{-1})
m	Feed discretization
N_i	Number of moles of reactant i (mol)
n	Revolution frequency (s^{-1})
n_b	Minimal revolution frequency of screws (s^{-1})
$\hat{\boldsymbol{n}}$	Direction unit vector
P_1, P_2	Products
P	Power (W)
Po	Power number ($Pd^{-5}n^{-3}\rho^{-1}$)
Q	Discharge flow (m^3 s^{-1})
Q_i	Volumetric flow of solution i (m^3 s^{-1})
q	Experimentally determined constant (m^3)
R_i	Reaction rate (mol s^{-1} m^{-3})
Re	Reynolds number for tank reactor ($nd^2\rho\mu^{-1}$)
Re_E	Reynolds number for extruder ($nd_E^2\rho\mu^{-1}$)
Re_{Eb}	Minimal Reynolds number for extruder ($n_b d_E^2 \rho\mu^{-1}$)
Sc	Schmidt number ($\mu\rho^{-1}D_A^{-1}$)
s	Striation thickness (m)
t	Time (s)
t_A	Feeding time of reactant A (s)
t_D	Characteristic diffusion time (s)
t_F	Characteristic deformation time (s)
t_M	Micromixing time (s)
t_R, t_{Ri}	Characteristic reaction times (s)
t_V	Time in which volume of reaction zone is doubled (s)
u_i	Velocity components in Lagrangian frame (m s^{-1})
$\vec{u}$	Velocity vector in Lagrangian frame (m s^{-1})
w_P	Weight fraction of polyethylenepolypropylene glycol
$\vec{X}$	Position of Lagrangian point (m)
X	Selectivity defined by Eq. (45)
x, y, z	Cartesian coordinates (m)
V	Volume of a spot of a tracer substance or reaction zone (m^3)
V_i	Volume of solution i (m^3)
v	Velocity (m s^{-1})
v_x, v_y, v_z	Velocity components (m s^{-1})
$\vec{v}$	Velocity vector (m s^{-1})

Greek letters

α	Rate of deformation (s^{-1})
α_i	Rate of deformation in the i direction (s^{-1})
α_{ij}	Angle between the old axis i and the new axis j (radians)
Γ	Dimensionless time defined by Eq. (50)
Δp	Overpressure (Pa)
δ_i	Penetration distance of tracer substance in the i direction (m)
ε	Rate of energy dissipation per unit volume ($kg\ m^{-1}\ s^{-3}$)
θ_I, θ_{II}, θ_{III}	Dimensionless time ratios defined by Eqs. (52), (53) and (61)
μ	Dynamic viscosity (Pa s)
ξ_i	Cartesian coordinate in Lagrangian frame (m)
$\boldsymbol{\xi}$	Position vector in Lagrangian frame (m)
ρ	Density ($kg\ m^{-3}$)
φ	$\varepsilon/\langle\varepsilon\rangle_V$
ψ	Dimensionless function of Reynolds number
ψ_E	Dimensionless constant
$\Omega_{i,j}$	Component of rotation tensor (s^{-1})
$\hat{\Omega}$	Rotation tensor (s^{-1})
ω	Angular velocity (s^{-1})

Subscripts

max	Maximal value
o	Initial value

Special symbols

$'$	Denotes variable in rotated frame of reference
$\overline{\quad}$	Mean value
$< >$	Environment variable
$\langle\rangle$	Time average
$\langle\langle\rangle\rangle$	Average over lifetime of limiting reactant and feeding time
$\langle\rangle_V$	Volume average

References

[1] S. Middleman, Fundamentals of Polymer Processing, McGraw-Hill, New York, 1977.
[2] Z. Tadmor, C.G. Gogos, Principles of Polymer Processing, Wiley-Interscience, New York, 1979.
[3] W. Mushick, Special Problems with Mixing Glass Melts by Stirres, 6th Eur. Conf. on Mixing, Pavia, Italy, May 1988, p. 527.
[4] M.A. Winkler, Problems in Fermenter Design and Operation, Chemical Engineering Problems in Biotechnology, Elsevier, Amsterdam, 1990.
[5] A. Tecante, L. Choplin, P.A. Tanguy, Hydrodynamics and Mass Transfer in Rheologically Complex Model of Exopolysaccharide Fermentation Broths, 7th Eur. Conf. on Mixing, Brugge, Belgium, September 1991, p. 367.
[6] J.B. Gray, Chem. Eng. Prog. 59 (1963) 55.
[7] C.J. Hoogendoorn, A.P. Hartog, Chem. Eng. Sci. 22 (1967) 1689.
[8] S. Nagata, Mixing Principles and Applications, Halsted, Wiley, New York, 1975.
[9] E.B. Nauman, B.A. Buffham, Mixing in Continuous Flow Systems, Wiley, Chichester, 1983.
[10] J. Bałdyga, J.R. Bourne, in: N.P. Cheremisinoff (Ed.), Encyclopedia of Fluid Mechanics, Vol. 1, Gulf Publishing, Houston, 1986, p. 145.
[11] J. Villermoux, in: N.P. Cheremisinoff (Ed.), Encyclopedia of Fluid Mechanics, Vol. 2, Gulf Publishing, Houston, 1986, p. 707.
[12] J. Bałdyga, R. Pohorecki, Chem. Eng. J. 58 (1995) 183.
[13] R.S. Spencer, R.M. Wiley, J. Coll. Sci. 6 (1951) 133.
[14] W.D. Mohr, R.L. Saxton, C.J. Jepson, Ind. Eng. Chem. 49 (1957) 1855.
[15] W.D. Mohr, in: E.C. Bernhardt (Ed.), Processing of Thermoplastic Materials, Reinhold Publishing, 1959, p. 117.
[16] W.E. Ranz, AIChE J., 25 (1979) 41.
[17] J.M. Ottino, W.E. Ranz, C.W. Macosko, Chem. Eng. Sci. 34 (1979) 877.
[18] J.M. Ottino, Chem. Eng. Sci. 35 (1980) 1377.
[19] J.M. Ottino, W.E. Ranz, C.W. Macosko, AIChE J. 27 (1981) 565.
[20] J.H. Tennekes, I.L. Lumley, A First Course in Turbulence, MIT Press, Cambridge, MA, 1972.
[21] N. Coburn, Vector and Tensor Analysis, Macmillan, New York, 1955.
[22] J. Bałdyga, J.R. Bourne, Chem. Eng. Sci. 45 (1990) 907.
[23] J. Bałdyga, Chem. Eng. Sci. 49 (1994) 1985.
[24] J.R. Bourne, S.-Y. Yu, Ind. Eng. Chem., Res. 33 (1994) 41.
[25] J.E. Crooks, in: C.H. Bamford, C.F.H. Tippers (Eds.), Comprehensive Chemical Kinetics, Vol. 8, Elsevier, Amsterdam, 1977, p. 209.
[26] A.J. Kirby, in: C.H. Bamford, C.F.H. Tippers (Eds.), Comprehensive Chemical Kinetics, Vol. 10, Elsevier, Amsterdam, 1972, p. 170.
[27] A. Rożeń, Investigation of Micromixing in Viscous Liquids, Ph.D. Thesis, Warsaw University of Technology, Warszawa, 1995.
[28] C.D. Denson, B.K. Hwang, SPE Tech. Papers, 26 (1980) 107.